

# Equilibrium Data for the $\text{N}_2\text{O}_5 + \text{HNO}_3 + \text{N}_2\text{O}_4$ System at 258.2 K, 265.2 K, 273.2 K, and 281.2 K

Zhiqiang Chen, Li Wang, Yonggang Zhu, Qingfa Wang,\* Xiangwen Zhang, and Zhentao Mi

Key Laboratory for Green Chemical Technology of State Education Ministry, School of Chemical Engineering and Technology, Tianjin University, Tianjin 30072, China

Liquid–liquid equilibrium data for the  $\text{N}_2\text{O}_5 + \text{HNO}_3 + \text{N}_2\text{O}_4$  system were measured by the cloud point method at 258.2 K, 265.2 K, 273.2 K, and 281.2 K. The solubility of dinitrogen pentoxide in dinitrogen tetroxide and nitric acid, dinitrogen tetroxide in nitric acid, and nitric acid in dinitrogen tetroxide and the tie lines were obtained separately. The single phase region, liquid–liquid equilibrium region, and liquid–solid equilibrium region were determined according to the equilibrium data. With the increase in temperature, the two-phase region reduces, and the solubilities of dinitrogen pentoxide in dinitrogen tetroxide and nitric acid, dinitrogen tetroxide in nitric acid, and nitric acid in dinitrogen tetroxide increase correspondingly.

## Introduction

Conventional nitrating agents normally involved nitric acid mixed with other reagents such as sulfuric acid in different proportions. During nitration, undesirable reactions and serious pollution often occurred. In addition, conventional nitration agents cannot be used for selective nitration and for deactivated substrates. Dinitrogen pentoxide ( $\text{N}_2\text{O}_5$ ) is an alternative nitrating agent. In contrast with the conventional nitrating agents, dinitrogen pentoxide has several advantages such as simple isolation of the product, easy control of temperature, and absence of spent acid for disposal.<sup>1,2</sup> Recently, dinitrogen pentoxide as a green nitrating agent has many applications in the nitration of organic compounds, particularly in the synthesis of energetic materials.<sup>3,4</sup>

Electrochemical synthesis of  $\text{N}_2\text{O}_5$  has been one of the main preparation methods.<sup>5</sup> At the end of electrolysis, the anolyte is a mixture of  $\text{N}_2\text{O}_5$ ,  $\text{HNO}_3$ , and  $\text{N}_2\text{O}_4$ , and the catholyte is a mixture of  $\text{H}_2\text{O}$ ,  $\text{HNO}_3$ , and  $\text{N}_2\text{O}_4$ . The solid-state  $\text{N}_2\text{O}_5$  can be obtained by separating and refining, usually using the crystallization method and the  $\text{N}_2\text{O}_4$  extraction method.<sup>6,7</sup> Obviously, these processes are based on the phase equilibrium data diagram of the  $\text{N}_2\text{O}_5 + \text{HNO}_3 + \text{N}_2\text{O}_4$  system. Therefore, it is necessary to study the  $\text{N}_2\text{O}_5 + \text{HNO}_3 + \text{N}_2\text{O}_4$  system and construct the phase diagram of this system.

In the  $\text{N}_2\text{O}_5 + \text{HNO}_3 + \text{N}_2\text{O}_4$  system,  $\text{N}_2\text{O}_5$  is easy to decompose. It is difficult for this system to obtain the equilibrium data by the static method, which requires a long time to reach the equilibrium.<sup>8</sup> Therefore, the cloud point method was used to obtain the equilibrium data for this system. Bagg et al. measured the equilibrium data of this system at (288.15 and 258.15) K. Rodgers et al.<sup>12</sup> measured the solubility of  $\text{N}_2\text{O}_4$  in  $\text{HNO}_3$  at (283.15 and 298.15) K. In this work, the cloud point method was also employed. The phase diagram of the ternary system was constructed and analyzed at 258.2 K, 265.2 K, 273.2 K, and 281.2 K.

## Experimental Section

**Chemicals.** Cerium(III) sulfate (A. R. purity > 99.5 %, Huabei Special Reagent, Huabei, China), ammonium ferrous sulfate

**Table 1.** Determination Results of  $\text{N}_2\text{O}_5$  (1) and  $\text{N}_2\text{O}_4$  (2) by the Titration and NMR Spectra, Separately<sup>9</sup>

no.	100 $w_2$	100 $w_1$	
		titration	NMR spectra
1	4.19	33.94	33.41
2	12.76	27.76	28.03

(A. R. purity > 99.5 %, Huabei Special Reagent), sodium hydroxide (A. R. purity > 99.5 %, Huabei Special Reagent, Huabei, China), concentrated nitric acid (purity > 99.8 %, Shandong Unite Chemical Industry, Shandong, China), and dinitrogen tetroxide (A. R. purity > 99.5 %, Jilin Chemical Industry, Jilin, China) were used without further purification.  $\text{N}_2\text{O}_5$  was prepared by the ozone method.<sup>1,6</sup> Double-distilled water was used in all experiments.

**Apparatus.** The experimental data for the ternary system were determined by the cloud point method under atmospheric pressure. The experimental apparatus included a jacketed glass vessel (internal volume about 50 cm<sup>3</sup>), a thermostatically bath, and a magnetic agitator. The measurement cell was placed in a temperature-controlled ethanol bath using thermostat (THD-3010, Ningbo, China). The temperature was maintained with precision of 0.1 K. All weights were carried out on a Libor AEG-220 balance (Germany) with a precision of 0.1 mg.

**Sample Analysis.** In our previous work, two analytic methods, including oxidation–reduction with acidity titration method and NMR spectrum with oxidation–reduction titration method, were developed to analyze the electrolyte.<sup>9</sup> In this work, the composition of the  $\text{N}_2\text{O}_5 + \text{HNO}_3 + \text{N}_2\text{O}_4$  system was also determined using the above methods. The results of these two methods coincide well (Table 1), and the uncertainty of measurement is 0.31 %. These results showed that the oxidation–reduction with the acidity titration method is credible. Therefore, the composition analysis of  $\text{N}_2\text{O}_4$ ,  $\text{N}_2\text{O}_5$ , and  $\text{HNO}_3$  was performed with a titration method. The reproducibility of this method was also investigated (Table 2), and the uncertainty of measurement is 0.55 %. The cerous sulfate solution, ammonium ferrous sulfate solution, and sodium hydroxide solution were prepared and calibrated according to the China national solution preparation criterion before experiment.<sup>13</sup>

\* Corresponding author. E-mail: qingfaw@yahoo.com.cn.

**Table 2. Results of Measurement Reproducibility of N<sub>2</sub>O<sub>5</sub> (1) and N<sub>2</sub>O<sub>4</sub> (2)**

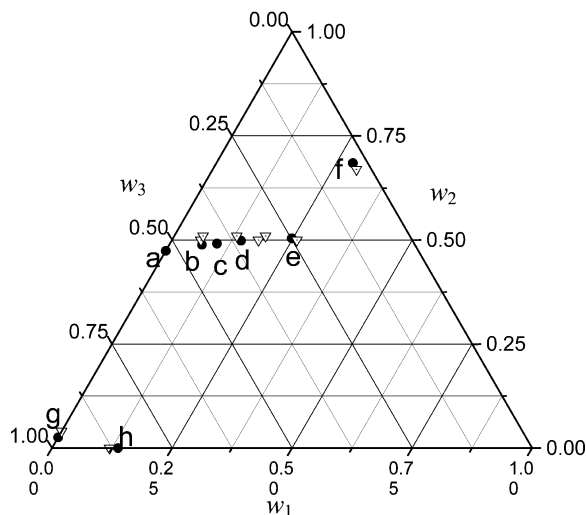
no.	100w <sub>1</sub>	100w <sub>2</sub>
1	28.38	9.65
2	28.55	9.70

**Solubility Measurement.** At the set temperature, A (N<sub>2</sub>O<sub>4</sub> or HNO<sub>3</sub>) of known mass was added to a glass vessel. B (N<sub>2</sub>O<sub>4</sub> or HNO<sub>3</sub> or N<sub>2</sub>O<sub>5</sub>) was then slowly added to the A solution under stirring, until the solution appeared to be cloudy. The addition of mass B was obtained by weight. The measurement cell was kept for complete phase separation. The liquid phase was sampled using a syringe. The composition was analyzed by titration.

**Equilibrium Data Measurement.** At the beginning of the experiments, N<sub>2</sub>O<sub>4</sub>, HNO<sub>3</sub>, and N<sub>2</sub>O<sub>5</sub> were added to the cell at known mass ratios. The weights of these reagents were determined by an electronic balance. The heterogeneous mixtures were stirred for 1 h at the set temperature and were then allowed to settle for (2 to 3) h for complete phase separation. Samples were carefully taken from the bottom HNO<sub>3</sub>-rich phase using the syringe. The composition of each sample was analyzed by titration.

## Results and Discussion

The liquid–liquid and liquid–solid equilibrium experimental data were compared with literature data,<sup>10,12</sup> as shown in Figure 1. It can be seen that the experimental data agreed well with equilibrium data in the literature. In Figure 1, the area above of points *a*, *b*, *c*, *d*, *e*, and *f* is the single liquid-phase region that was rich in HNO<sub>3</sub>; the area below *g* and to the left of *h* is the single liquid-phase region that was rich in N<sub>2</sub>O<sub>4</sub>; the area between the above single liquid-phase areas is the liquid–liquid phase region; the rest of the area on the right angle of the triangular phase diagram is the liquid–liquid–solid phase region. For liquid–liquid equilibrium experiment, points *a*, *b*, *c*, *d*, and *e* were the composition of the bottom layer (HNO<sub>3</sub>-rich phase). Point *f* of the solubility of N<sub>2</sub>O<sub>5</sub> in HNO<sub>3</sub> should be in the liquid–solid line. For decomposition of N<sub>2</sub>O<sub>5</sub>, the N<sub>2</sub>O<sub>4</sub> existed in the experiment of N<sub>2</sub>O<sub>5</sub> solubility in HNO<sub>3</sub>. The fact resulted in the deviation of point *f* from the edge line of the triangular phase diagram. Points *g* and *h* were the solubility of N<sub>2</sub>O<sub>4</sub> in HNO<sub>3</sub> and the solubility of N<sub>2</sub>O<sub>5</sub> in N<sub>2</sub>O<sub>4</sub>, respectively.

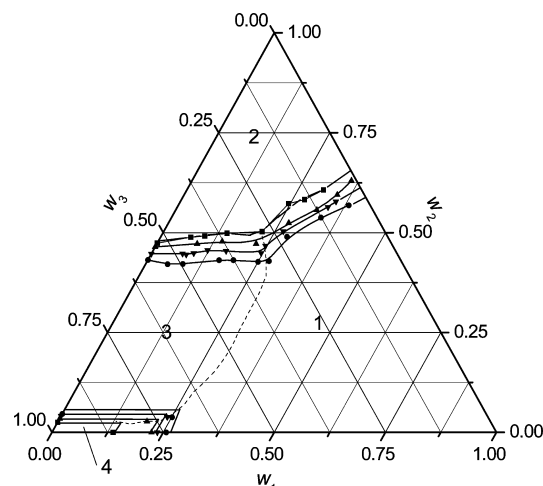
**Figure 1.** Equilibrium data of the N<sub>2</sub>O<sub>5</sub> (1) + HNO<sub>3</sub> (2) + N<sub>2</sub>O<sub>4</sub> (3) system at 258.2 K: ●, experimental data; ▽, literature data.**Table 3. Liquid–Liquid Equilibrium Data of the N<sub>2</sub>O<sub>5</sub> (1) + HNO<sub>3</sub> (2) + N<sub>2</sub>O<sub>4</sub> (3) System from T = (265.2 to 281.2) K As a Function of Mass Fraction, w<sub>1</sub>, w<sub>2</sub>, at Atmospheric Pressure**

T/K = 258.2		T/K = 265.2		T/K = 273.2		T/K = 281.2	
100 w <sub>1</sub>	100 w <sub>2</sub>	100 w <sub>1</sub>	100 w <sub>2</sub>	100 w <sub>1</sub>	100 w <sub>2</sub>	100 w <sub>1</sub>	100 w <sub>2</sub>
0.00	47.37	0.00	46.45	0.00	4.47	0.00	43.15
6.77	48.87	6.99	44.78	6.99	44.77	4.95	42.08
9.77	49.16	7.93	44.53	7.93	44.53	8.35	42.17
14.48	49.86	9.04	47.21	9.44	44.90	16.06	43.10
24.74	50.41	14.41	47.78	12.24	45.58	19.24	43.12
24.60	57.28	26.57	48.71	16.50	45.41	25.03	42.698
30.72	60.71	35.87	63.02	24.62	44.88	27.39	42.89
22.15	50.29	34.46	59.46	24.71	46.70	38.33	56.87
0.00	2.57	27.06	52.40	26.89	50.33	33.63	53.79
13.75	0.00	31.75	55.64	33.90	56.39	28.38	48.95
27.69	58.28	22.37	47.17	0.00	4.12	0.00	4.63
		20.54	0.00	24.00	3.87	25.12	3.78
		0.00	3.46	24.54	4.01	25.71	0.00
		20.01	2.74	23.69	0.00		
				35.01	57.81		

**Table 4. Tie-Lines Data of the N<sub>2</sub>O<sub>5</sub> (1) + HNO<sub>3</sub> (2) + N<sub>2</sub>O<sub>4</sub> (3) System from T = (265.2 to 281.2) K As a Function of Mass Fraction, w<sub>1</sub>, w<sub>2</sub>, at Atmospheric Pressure**

T/K	no.	overall		bottom phase	
		100 w <sub>1</sub>	100 w <sub>2</sub>	100 w <sub>1</sub>	100 w <sub>2</sub>
258.2	1	9.13	25.50	7.87	48.62
	2	5.70	30.93	5.75	49.03
	3	13.40	26.61	13.91	48.73
	4	8.38	31.78	10.28	49.58
265.2	1	9.80	27.00	8.84	45.63
	2	10.60	28.15	11.25	46.25
	3	13.00	30.17	12.81	46.74
	4	5.09	29.77	3.70	44.96
	5	7.17	30.62	6.62	47.13
	6	15.83	27.62	15.97	47.95
273.2	1	19.51	29.24	18.79	44.32
	2	16.34	34.12	14.35	44.70
	3	18.58	4.04	5.45	43.87
	4	9.70	32.54	8.21	44.12
	5	9.22	27.60	11.29	45.63
281.2	1	6.66	25.22	9.88	41.32
	2	19.35	31.86	22.25	41.93
	3	4.59	31.96	6.93	41.17
	4	11.23	27.54	13.38	42.15
	5	17.02	27.14	16.04	42.17

The solubility and equilibrium data for the ternary system, N<sub>2</sub>O<sub>5</sub> + HNO<sub>3</sub> + N<sub>2</sub>O<sub>4</sub> are listed in Tables 3 and 4. The

**Figure 2.** Phase diagram of the N<sub>2</sub>O<sub>5</sub> (1) + HNO<sub>3</sub> (2) + N<sub>2</sub>O<sub>4</sub> (3) system: ●, 258 K; ▲, 265.2 K; ▼, 273.2 K; ■, 281.2 K; 1, the N<sub>2</sub>O<sub>5</sub>(s) + HNO<sub>3</sub>(l) + N<sub>2</sub>O<sub>4</sub>(l) region; 2, the HNO<sub>3</sub>(l) region; 3, the HNO<sub>3</sub>(l) + N<sub>2</sub>O<sub>4</sub>(l) region; 4, the N<sub>2</sub>O<sub>4</sub>(l) region.

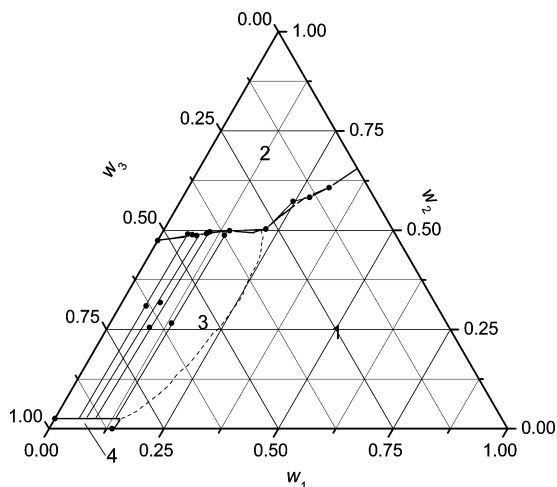


**Figure 3.** Tie-line diagram of the  $\text{N}_2\text{O}_5(1) + \text{HNO}_3(2) + \text{N}_2\text{O}_4(3)$  system at 258.2 K: 1, the  $\text{N}_2\text{O}_5(\text{s}) + \text{HNO}_3(\text{l}) + \text{N}_2\text{O}_4(\text{l})$  region; 2, the  $\text{HNO}_3(\text{l})$  region; 3, the  $\text{HNO}_3(\text{l}) + \text{N}_2\text{O}_4(\text{l})$  region; 4, the  $\text{N}_2\text{O}_4(\text{l})$  region.

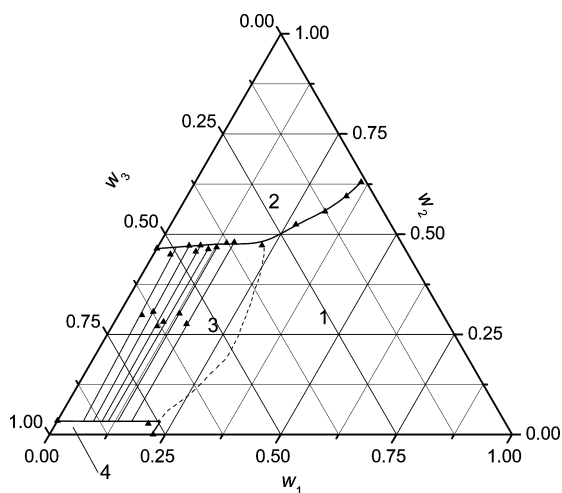


**Figure 4.** Tie-line diagram of the  $\text{N}_2\text{O}_5(1) + \text{HNO}_3(2) + \text{N}_2\text{O}_4(3)$  system at 265.2 K: 1, the  $\text{N}_2\text{O}_5(\text{s}) + \text{HNO}_3(\text{l}) + \text{N}_2\text{O}_4(\text{l})$  region; 2, the  $\text{HNO}_3(\text{l})$  region; 3, the  $\text{HNO}_3(\text{l}) + \text{N}_2\text{O}_4(\text{l})$  region; 4, the  $\text{N}_2\text{O}_4(\text{l})$  region.

triangular phase diagrams of the ternary system are shown in Figures 2, 3, 4, 5, and 6. When the temperature increased from (258.5 to 281.2) K, the mass fraction of  $\text{N}_2\text{O}_4$  in  $\text{HNO}_3$ ,  $\text{N}_2\text{O}_5$  in  $\text{HNO}_3$ ,  $\text{HNO}_3$  in  $\text{N}_2\text{O}_4$ , and  $\text{N}_2\text{O}_5$  in  $\text{N}_2\text{O}_4$  increased from 52.63 %, 28.42 %, 2.57 %, and 13.75 % to 56.85 %, 33.38 %, 4.63 %, and 25.71 %, respectively. It can be seen from these results that the temperature has a much more evident influence on the solubility of  $\text{N}_2\text{O}_5$  in  $\text{N}_2\text{O}_4$  than  $\text{N}_2\text{O}_5$  in  $\text{HNO}_3$ .

The intersection of the liquid–solid lines and liquid–liquid lines were the critical points. In these points, the mass fraction of  $\text{N}_2\text{O}_5$  was 24.74 %, 26.57 %, 24.62 %, and 19.24 % at 258.2 K, 265.2 K, 273.2 K, and 281.2 K, respectively. In Figures 2, 3, 4, 5, and 6, the dashed lines that connect these points delegate the critical line. The single-phase region, liquid–liquid equilibrium region, and liquid–solid equilibrium region were determined according to the equilibrium data. When the system was in the liquid–liquid equilibrium region, the system was separated into two phases. The compositions of two phases were in liquid–liquid lines according to the tie line data. The facts can be helpful for selecting better experimental conditions in crystallization and

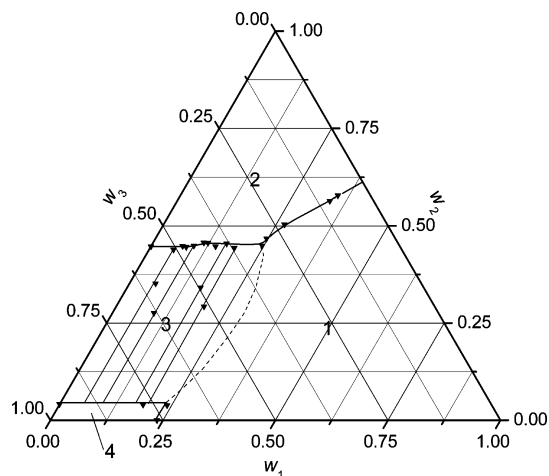


**Figure 5.** Tie-line diagram of the  $\text{N}_2\text{O}_5(1) + \text{HNO}_3(2) + \text{N}_2\text{O}_4(3)$  system at 273.2 K: 1, the  $\text{N}_2\text{O}_5(\text{s}) + \text{HNO}_3(\text{l}) + \text{N}_2\text{O}_4(\text{l})$  region; 2, the  $\text{HNO}_3(\text{l})$  region; 3, the  $\text{HNO}_3(\text{l}) + \text{N}_2\text{O}_4(\text{l})$  region; 4, the  $\text{N}_2\text{O}_4(\text{l})$  region.

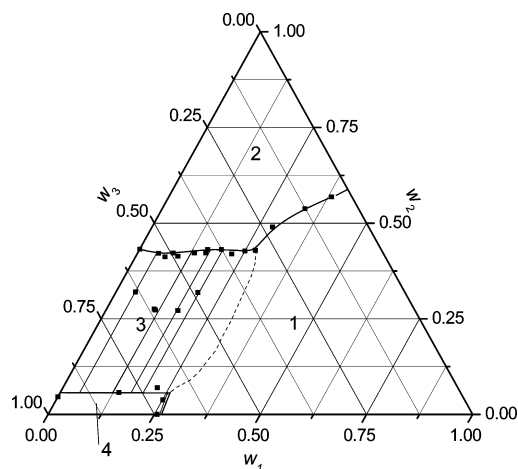


**Figure 6.** Tie-line diagram of the  $\text{N}_2\text{O}_5(1) + \text{HNO}_3(2) + \text{N}_2\text{O}_4(3)$  system at 281.2 K: 1, the  $\text{N}_2\text{O}_5(\text{s}) + \text{HNO}_3(\text{l}) + \text{N}_2\text{O}_4(\text{l})$  region; 2, the  $\text{HNO}_3(\text{l})$  region; 3, the  $\text{HNO}_3(\text{l}) + \text{N}_2\text{O}_4(\text{l})$  region; 4, the  $\text{N}_2\text{O}_4(\text{l})$  region.

$\text{N}_2\text{O}_4$  extraction processes. When the equilibrium system exceeded the critical line, the yellow precipitation (the solid  $\text{N}_2\text{O}_5$ ) appeared instantly. The lower the temperature was, the more evident this phenomenon was.

## Conclusions

The solubility, liquid–liquid, and liquid–solid equilibrium data for the  $\text{N}_2\text{O}_5 + \text{HNO}_3 + \text{N}_2\text{O}_4$  system are reported at four temperatures and atmospheric pressure. From the results, the two-phase region diminished and the solubility increased with increasing temperature. At 258.15 K, 265.2 K, 273.2 K, and 281.2 K, the mass fraction of  $\text{N}_2\text{O}_5$  was 24.74 %, 26.57 %, 24.62 %, and 19.24 % in the critical points of the liquid–solid curve.

**Note Added after ASAP Publication:** This paper was published ASAP on April 27, 2009. The corresponding author was changed. The revised paper was reposted on April 29, 2009.

## Literature Cited

- (1) Latypov, N. V.; Wellmar, U.; Goede, P.; Bellamy, A. J. Synthesis and Scale-Up of 2,4,6,8,10,12-Hexanitro-2, 4,6,8,10,12-hexaazaisowurtzitane from 2,6,8,12-Tetraacetyl-4,10-dibenzyl-2,4,6,8,10,12-hexaazaisowurtzitane (HNIW, CL-20). *Org. Process. Res. Dev.* **2000**, *4*, 156–158.

- (2) Zhang, M. A.; Eaton, E.; Gilardi, R. Hepta and Octanitrocubanes. *Angew. Chem., Int. Ed.* **2000**, 39, 401–404.
- (3) Talawar, M. B.; Sivabalan, R. Establishment of Process Technology for the Manufacture of Dinitrogen Pentoxide and Its Utility for the Synthesis of Most Powerful Explosive of Today: CL-20. *J. Hazard. Mater.* **2005**, 124, 153–164.
- (4) Feuer, H.; Nielsen, A. T. *Nitro Compounds*; Purdue University Press: West Lafayette, IN, 1990.
- (5) Agrawal, J. P.; Hodgson, R. D. *Organic Chemistry of Explosives*; John Wiley & Sons: Chichester, U.K., 2007.
- (6) Kargin, Y. M.; Chichirov, A. A.; Parakin, O. V. *Method for Preparing Nitrogen Pentoxide*. U.S. Patent 1,089,047, April 30, 1984.
- (7) Bagg, G. E.; Salter, D. A. *Method of Separating Dinitrogen Pentoxide from Its Solution in Nitric Acid*. Britain Patent GB 2245266, January 02, 1991.
- (8) Swinton, P.; Rodgers, M. J.; Bagg, G. E. G. *Solvent Transfer Process for Dinitrogen Pentoxide*. China Patent GB 2293833, April 01, 1994.
- (9) Zhang, J.; Wang, L.; Su, M. The Analytic Method for N<sub>2</sub>O<sub>4</sub> and N<sub>2</sub>O<sub>5</sub> in Anhydrous HNO<sub>3</sub>. *Energ. Mater.* **2006**, 14, 62–65.
- (10) Swinton, P. E.; Rodgers, M. J.; Bagg, G. E. G. *Solvent Transfer Process for Dinitrogen Pentoxide*. German Patent DE 69412482, November 24, 1994.
- (11) Bagg, G. E. Q.; Salter, D. A. *Method of Separating Electrochemically Produced Dinitrogen Pentoxide from Its Solution in Nitric Acid*. U.S. Patent 5,128,001, January 02, 1992.
- (12) Rodgers, M. J.; Swinton, P. E. Isolation of Electrochemically Generated Dinitrogen Pentoxide in a Pure Form and Its Use in Aromatic Nitrations. In *Nitration: Recent Laboratory and Industrial Developments*; Albright, L. F., Carr, R. V. C., Schmitt, R. J., Eds.; ACS Symposium Series 623; American Chemical Society: Washington, D.C., 1996; p 58.
- (13) Hao, Y. L. *Preparations of Standard Volumetric Solutions*; Standards Press of China: Beijing, 2003.

Received for review December 17, 2008. Accepted April 10, 2009. We thank the state education ministry for supplying financial support on this work.

JE800971F